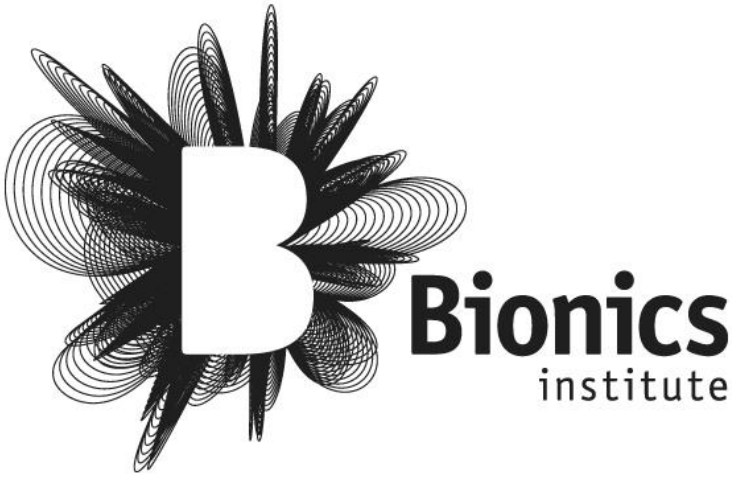

Evaluation of stimulus parameters and electrode geometry for an effective suprachoroidal retinal prosthesis

Running Head: Evaluation of a suprachoroidal retinal prosthesis

Mohit N Shivdasani[1], Chi D Luu[2], Rosemary Cicione[1,4], James B Fallon[1], Penny J Allen[2], James Leuenberger[1], Gregg J Suaning[3], Nigel H Lovell[3], Robert K Shepherd[1] and Chris E Williams[1]

[1]The Bionic Ear Institute, Daly Wing, St Vincent's Hospital, VIC – 3065, AUSTRALIA

[2]Centre for Eye Research Australia, University of Melbourne, Royal Victorian Eye & Ear Hospital, VIC – 3002, AUSTRALIA

[3]Graduate School of Biomedical Engineering, University of New South Wales, NSW – 2052, AUSTRALIA

[4]Department of Electronic Engineering, La Trobe University, VIC – 3086, AUSTRALIA

Corresponding Author:

Dr. Mohit N. Shivdasani

The Bionic Ear Institute, 6th Floor, Daly Wing, St Vincent's Hospital, Fitzroy, VIC – 3065, AUSTRALIA.

Tel: +61-3-92883525

Fax: +61-3-92882998

Email: mshivdasani@bionicear.org

Abstract:

Several approaches have been proposed for placement of retinal prostheses; epiretinal, sub-retinal, and suprachoroidal. We aimed to systematically evaluate the effectiveness of varying a range of stimulus parameters and electrode geometry for a suprachoroidal electrode array, using cortical evoked responses to monopolar electrical stimulation in cats. Our results indicate that charge thresholds were not dependent on electrode size, pulse widths or position of the return electrode tested, but were dependent on the number of sites stimulated in parallel. Further, we found that the combination of monopolar stimulation with large diameter electrodes, wide pulse widths and parallel stimulation minimized the voltage requirements for stimulation. These results provide useful insights for the design specifications of a low voltage suprachoroidal stimulator.

Introduction:

It is anticipated that a retinal prosthesis will restore a sense of vision in patients afflicted with retinal degenerative disorders such as retinitis pigmentosa and age-related macular degeneration. A retinal prosthesis will bypass the damaged photoreceptive layer and electrically stimulate subsequent retinal layers. Current human research predominantly focuses on two main sites for implantation of the electrode array; epiretinal and subretinal. Epiretinal prostheses are positioned in the vitreous cavity of the eye and directly stimulate the inner retina. The close proximity of the electrode array with the target retinal ganglion cells should result in lower thresholds for activation compared to electrodes placed in alternative anatomical positions (de Balthasar *et al* 2008). However, stable attachment of the array to the inner retinal surface has proven to be problematic (Majji *et al* 1999). Fundus images along with optical coherence tomography measurements taken during clinical trials have shown movement of the array away from the retinal surface (de Balthasar *et al* 2008). An alternative approach consists of a subretinal placement of a microphotodiode array, offering more mechanical stability than the epiretinal approach and theoretically replacing the function of the photoreceptors. However, the implant is known to obstruct metabolic support from the choroidal vasculature resulting in the risk of further retinal damage including disorganization of the inner nuclear layers (Chow *et al* 2001).

Problems associated with the epiretinal and subretinal approaches have driven the development of the suprachoroidal implant, the feasibility of which was first demonstrated in normal and blind rats (Kanda *et al* 2004). The suprachoroidal electrode array is inserted between the sclera and choroid through a simple scleral incision and remains isolated from the retina, thereby mitigating the risk of retinal damage (Nakauchi *et al* 2005). The suprachoroidal implant has the added advantage of a simple surgery (Nakauchi *et al* 2005, Zhou *et al* 2008) and long term studies show stable electrode positioning in the suprachoroidal space (Zhou *et al* 2008). However, given the distance between the retina and sclera (approximately 250-300 μm in cats; 204-490 μm in humans, Brown *et al* 2009), it has been suggested that a suprachoroidal prosthesis will not

achieve as high resolution as epiretinal or subretinal prostheses (Kanda *et al* 2004). In addition, higher currents may be required to stimulate the retina, though recent studies in normally sighted animals show that cortical potentials can be reliably evoked using suprachoroidal stimulation (Nakauchi *et al* 2005, 2007, Wong *et al* 2008, 2009, Kanda *et al* 2004, Sakaguchi *et al* 2004). Preliminary studies in two subjects with retinitis pigmentosa have confirmed that suprachoroidal stimulation is able to induce phosphenes (Fujikado *et al* 2007). In the present study, using the cat as an animal model, our aim was to evaluate the effectiveness of varying electrode geometry and a range of stimulus parameters with suprachoroidal stimulation. Specifically, we aimed to characterize the dependence of electrode impedance and thresholds required for cortical activation on electrode size, pulse width, number of electrode sites stimulated in parallel and the site of return electrode placement for electrical stimulation.

Materials and Methods:

Anaesthesia and Surgery

These studies were approved by the Royal Victorian Eye and Ear hospital animal ethics committee. Acute experiments were performed over a period of three days. Normally-sighted adult cats (n = 5) weighing between 3.8-5.2 kgs were anaesthetized with an initial dose of Ketamine (intramuscular, i.m., 20 mg/kg) and Xylazine (subcutaneous, s.c., 2 mg/kg), followed by continuous slow intravenous infusion of Sodium Pentobarbitone (60 mg/ml, 1:6 dilution). In addition, animals were treated with dexamethasone (i.m., 0.1 mg/kg) and clavulox (s.c., 10 mg/kg) at regular intervals throughout the experiment. A slow continuous intravenous infusion of Hartmann's solution (sodium lactate, 1.5 mg/ml/hr) was administered throughout the experiment. Respiration rate, end-tidal CO_2 and core body temperature (37 ºC) were monitored and maintained within normal levels (Fallon *et al* 2009). Pupils were dilated by topical application of a mixture of phenylephrine hydrochloride (10%) and tropicamide (1%). The surgery consisted of a temporal approach, with a lateral canthotomy followed by a full-thickness incision through the sclera to expose the choroid. A "pocket" was made with a blade within the suprachoroidal space. A flexible electrode array (details below) was inserted 15-17 mm into each eye (total of 10 eyes) beneath the area centralis in the suprachoroidal space by an experienced retinal surgeon (Allen, P.J.). The array was anchored with sutures to the sclera (Allen *et al* 2009). Platinum ball electrodes (1.5 mm diameter) were implanted into the vitreous humour and the suprachoroidal space (adjacent to the electrode array) to act as return electrodes for electrical stimulation. The animal was placed in a stereotaxic frame (David Kopf Instruments, Tujunga, CA) and kept in a dark, electrically shielded Faraday room. A platinum reference electrode used for all recordings was implanted in a skin fold at the back of the neck. Following visual assessment of the eye, a craniotomy was performed to expose the primary visual cortex. A platinum macro-electrode was placed on the surface of the visual cortex close to the posterior lateral gyrus, corresponding to the macular region of the retina (Tusa *et al* 1978). This electrode was used for all evoked potential

recordings in response to full-field flashes (Espion Systems, Diagnosys, LLC, MA) and electrical stimulation (details below) of the suprachoroidal electrode array. In one experiment, a single tungsten microelectrode (World Precision Instruments, Sarasota, FL) was inserted into the visual cortex to record multiunit activity in response to both visual flash and electrical stimulation.

Suprachoroidal Electrode Array

The suprachoroidal electrode array (figure 1) was designed in-house and manufactured through Flexible Circuit Technologies (Plymouth, MN) using a flexible polyimide substrate (25µm thick). The arrays were specifically designed for use in acute studies only. Electrode sites and circuit tracks were initially made of copper (12 µm thick) and a suitable solder mask (15-18 µm) was used to cover the whole substrate leaving only the electrode sites exposed. The exposed sites were first electroplated with Nickel (1-3 µm), followed by Gold (0.1 µm), then Platinum (1 µm). Electrode sites were arranged in a 6 row x 12 site configuration (figure 1B). The spacing between rows was 0.8 mm and site spacing on each row was 1 mm (approximately 4º visual angle in cats, Hubel and Wiesel 1959; 3.5º visual angle in humans, Drasdo and Fowler 1974). Each row had electrode sites that were of different sizes with 160 µm diameter sites (2.01×10^{-4} cm^2 geometric surface area) on rows 1-3 and row 5, 125 µm diameter sites (1.23×10^{-4} cm^2 geometric surface area) on row 4, and 395 µm diameter sites (1.23×10^{-3} cm^2 geometric surface area) on row 6 (figure 1B). Prior to implantation, the electrode array (except connectors and electrode sites) and 1 mm surrounding edges were coated with Silicone (Permatex, CT; Type 65AR flowable; 150-400 µm tapered thickness from tip).

Stimulation and Recording Paradigms

Suprachoroidal electrode arrays were connected to a 512 cross-point switch matrix (PXI 2532, National Instruments, Austin, TX) configured as a 4 x 128 multiplexer (Leuenberger *et al* 2008). Two input channels of the multiplexer were connected to an isolated constant current stimulator

and two channels were used to monitor and record the voltage across the electrodes using a Digital Multimeter (PXI 4072, National Instruments, Austin, TX). Each output channel of the multiplexer was connected to an electrode site on the array, thereby enabling simultaneous addressing of multiple electrode sites. Automated impedance monitoring software was developed in LabView (National Instruments, Austin, TX) to measure the impedance of each electrode site on the array. Impedance measurements were performed *in vitro* prior to implantation in a saline bath, immediate post-op *in vivo* and in the morning of each recording day (approximately 16 hours and 40 hours post-op). For impedance measurements, a single constant current cathodic-leading biphasic charge-balanced pulse (100 µA, 250 µs per phase for 125 µm diameter sites; 200 µA, 250 µs per phase for 160 µm and 395 µm diameter sites) was delivered to each electrode site and the induced voltage waveform was recorded (examples in figure 2, maximum stimulator compliance voltage of 24 volts). Impedance was calculated as the maximum peak of the leading cathodic phase of the induced voltage divided by the current (Xu *et al* 1997). Impedance measurements and all other electrical stimulation paradigms were performed in a monopolar configuration with either the vitreous or suprachoroidal ball electrode (350 Ω measured impedance) used as the return.

Evoked potentials from the surface of the visual cortex elicited by full-field flashes (0.0~~0~~01-3 cd.s/m^2) and cathodic-leading biphasic charge-balanced current pulses (0-2 mA, 100-500 µs per phase, most recordings with 500 µs per phase) were recorded (National Instruments data acquisition card NI USB-6251, 10-2000 Hz bandpass filtered, 100 kHz sampling rate) via the platinum macro-electrode. In one animal, multiunit spike activity (300-6000 Hz bandpass filtered) was recorded using a tungsten microelectrode. To detect spikes an estimate of the background noise level (without electrical stimulation) was made by calculating the root mean square (RMS) value of the incoming signal. Multiunit spikes were detected and time-stamped when the signal was found to exceed 4.2 times the RMS value. Visual and electrical stimulation were performed at a rate of 1 Hz. An ensemble averaged response was recorded over a total of 25 trials at each

stimulus intensity. Each input-output function was repeated to ensure consistent recordings. Electrical stimulation was predominantly performed on full rows (all 12 electrode sites on a row connected in parallel to the stimulator), half-rows (first six electrode sites from tip connected in parallel to the stimulator) and single electrode sites. To assess the effect of parallel stimulation of multiple sites within a row, the number of sites connected in parallel to the stimulator was varied between 1 and 12 sites from the tip. This technique of multiplexing would result in current division through each of the electrode sites connected in parallel, as determined by their individual impedances. The stimulus current for each input-output function was increased in 100 or 200 µA steps from 0 µA to a maximum current of either 2 mA or the current that yielded a maximum charge density of 300 $\mu C/cm^2$ per phase. The charge density limit was applied to ensure that the electrodes were not operated above known gassing limits for Pt electrodes (Brummer and Turner 1977). For each averaged response, the peak (maxima) and trough (minima) were calculated 2-30 ms from stimulus onset without the presence of the stimulus artefact (shaded region in figure 5). The threshold for each evoked response was defined as the current that yielded positive-going peaks within 30 ms from stimulus onset of at least 0.3 mV (figure 5). Thresholds were calculated as total charge (µC, current multiplied by pulse width). In addition, the slope of each response amplitude-current intensity input-output function (figure 5) was determined.

Histology

At the end of the experiment, animals were deeply anaesthetized using an overdose of Sodium Pentobarbitone (150 mg/kg, intra-peritoneal) and perfused transcardially using heparinized saline at 37 ºC and 4% paraformaldehyde (PFA) at 4 ºC. The eyes were removed for histology and kept in 4% PFA for post fixing. Gross anatomical and histological assessments were made prior to sectioning (Allen *et al* 2009). Detailed histological results have been submitted for publication elsewhere.

Statistical Analyses

Analyses were performed on impedance, thresholds and input-output function slopes, and compared across different; return electrodes (suprachoroidal versus vitreous), electrode sizes, numbers of sites stimulated in parallel and pulse widths. All statistical analyses were performed using PASW Statistics 17 (SPSS Inc., Chicago, IL). Immediate post-op *in vivo* impedances were compared to *in vitro* impedances using independent sample t-tests for the three electrode sizes. A two-way univariate ANOVA was performed to analyze interactions between time after implantation *in vivo* and electrode size, on impedance. Mann-Whitney U tests were used to assess the significance of the site of return electrode placement on cortical thresholds. Two-way univariate ANOVAs were performed to analyse interactions between number of stimulated sites in parallel and electrode size on cortical thresholds, amplitude gradients and latency gradients. Finally, the effects of pulse widths on charge thresholds were analyzed using linear regression. All values reported are *Mean* ± *Standard Error of Mean*.

Results:

Electrode Impedance

Figure 2 shows voltage waveforms for the various electrode sizes recorded during impedance measurements *in vitro* and approximately 40 hours post-op *in vivo* using the vitreous return. Impedances were calculated as the peak of the induced voltage of the leading cathodic phase divided by the peak injected current during the same phase. Figure 3 depicts electrode impedance recorded in saline (*in vitro*) and as a function of time after implantation (*in vivo*), for electrode sites with different diameters (data from both return electrodes combined). Independent sample t-tests were performed on *in vivo* impedance data at each time point after implantation to assess the effect of return placement. Impedance recorded *in vivo* for the 125 µm diameter electrode sites using the suprachoroidal return were significantly higher (immediate post-op, $p < 0.01$; 16 hours post-op, $p < 0.001$; 40 hours post-op, $p < 0.005$) than those using the vitreous return. For the 160 µm and 395 µm diameter electrode sites, impedances using the vitreous return were not significantly different ($p > 0.05$) from those using the suprachoroidal return.

Independent samples t-tests were performed to compare impedances recorded *in vitro* and immediate post-op *in vivo*. For all electrode sizes, impedances recorded immediately post-op *in vivo* (125 µm, 46.8±1.3 kΩ; 160 µm, 33.1±0.4 kΩ; 395 µm, 14.6±0.5 kΩ) were on average 2.5-4 times larger ($p < 0.001$) than those recorded *in vitro* (125 µm, 16.5±0.6 kΩ; 160 µm, 14.8±0.6 kΩ; 395 µm, 7.7±1.0 kΩ). A 3 (time after implantation: immediate post-op, 16 hours post-op and 40 hours post-op) x 3 (electrode size: 125 µm diameter, 160 µm diameter and 395 µm diameter) univariate ANOVA was performed to analyze the effects of time after implantation and electrode size on impedance. A significant interaction effect was found between time after implantation and electrode size [$F(4,2218) = 5.65$, $p < 0.0001$, $\eta^2 = 0.01$]. Follow-up simple effects analysis of time after implantation showed different effects for the various electrode sizes. For the smallest electrode sites with 125 µm diameter, impedances recorded 16 hours post-op (51.5±1.3 kΩ) and 40 hours post-op (51.4±1.2 kΩ) were significantly different from those recorded immediate post-

op (figure 3), but were not significantly different from each other. A similar pattern was observed for electrode sites with 160 μm diameter (figure 3; 16 hours post-op, 36.9±0.4 kΩ; 40 hours post-op, 37.3±0.3 kΩ). For the largest electrode sites with 395 μm diameter, impedances progressively increased as a function of time with 16 hours post-op values (20±0.6 kΩ) larger than those recorded immediate post-op and 40 hours post-op values (24.5±0.6 kΩ) larger than those recorded at both immediate post-op and 16 hours post-op (figure 3). As expected, electrode size also influenced impedance. Follow-up simple effects analysis of electrode size showed that at all time points during the experiments, impedances of the 125 μm diameter electrode sites were larger than those of the 160 μm diameter electrode sites, which in turn were larger than those of the 395 μm diameter electrode sites (figure 3).

Cortical Evoked Responses

Reproducible evoked responses were recorded in response to visual and electrical stimulation in seven of ten eyes. In three eyes, excessive haemorrhage was encountered either during surgery (n = 1, unable to implant array) or after implantation of the electrode array (n = 2, no responses obtained to electrical stimulation). In the remaining seven eyes cortical responses were consistent over the duration of the experiments and across animals. Responses evoked by both visual and electrical stimulation typically consisted of a single positive peak followed by a negative trough, latencies of which depended on the type and intensity of the stimulus (figure 4). Both visual flashes (not illustrated) and electrical stimulation (figure 5) elicited responses that monotonically increased in amplitude with increasing stimulus intensities. With visual stimulation, the latencies of the positive peaks of the evoked responses decreased with increasing flash intensity (20-30 ms at maximum brightness of 3cd/m^2). In contrast, for electrical stimulation, response latencies did not change with increased current (figure 5, 7.7±0.3 ms at threshold, 7.7±0.3 ms at maximum stimulus current used).

Cortical Thresholds

It was generally easier to activate the visual cortex within our defined maximum charge density/current limits, by stimulating full rows of 12 electrode sites on the suprachoroidal array compared to half-rows (first 6 electrode sites from tip) and single electrode sites, particularly for smaller electrode sizes. Stimulation of full rows of 125 μm electrode sites was able to elicit a response in three of the seven eyes using a 500 μs pulse width (0.35±0.03 μC threshold). It was not possible to evoke discernable cortical responses when stimulating the 125 μm electrode sites as either half-rows or single electrode sites. Further, the 160 μm electrode sites were able to elicit discernable responses from stimulation of full rows and half-rows in all seven eyes, while activation of a single 160 μm site was effective in only one eye with a threshold close to the maximum charge density (298.42 μC/cm^2 per phase). Finally, sites with 395 μm diameter were able to elicit clearly discernable responses when stimulated as full rows, half-rows and single electrode sites in all seven eyes within the maximum stimulus intensity limits.

Effect of Return Electrode Placement:

To analyze the effects of return placement, electrode size and the number of sites stimulated in parallel within a row on cortical thresholds, all statistics were performed on threshold data using a pulse width of 500 μs and for the 160 μm (rows and half-rows) and 395 μm (rows, half-rows and single) diameter electrode sites from seven eyes. The position of the return electrode for electrical stimulation did not affect cortical thresholds (Mann-Whitney U test, $p > 0.05$). This effect was observed for stimulation of both rows (suprachoroidal return, 11 rows in 4 eyes, 0.44±0.02 μC; vitreous return, 28 rows in 7 eyes, 0.44±0.02 μC) and half-rows (suprachoroidal return, 8 half-rows in 5 eyes, 0.24±0.02 μC; vitreous return, 16 half-rows in 6 eyes, 0.23±0.02 μC) of the 160 μm electrode sites. Further, for stimulation of sites with 395 μm diameter, this effect was observed for stimulation of rows (suprachoroidal return, 1 row from 1 eye, 0.4 μC; vitreous return, 6 rows in 6 eyes, 0.3±0.07 μC), half-rows (suprachoroidal return, 1 half-row in 1 eye, 0.4 μC; vitreous return, 7 half-rows in 7 eyes, 0.17±0.04 μC) and single sites (suprachoroidal return,

2 sites in 2 eyes, 0.13±0.03 µC; vitreous return, 12 sites in 7 eyes, 0.14±0.02 µC). Since cortical thresholds were not affected by return electrode placements, for all further analyses, threshold data from both return placements were pooled.

Effect of Electrode Size & Number of Sites Stimulated in Parallel within a Row:

Figure 6 shows changes in cortical thresholds in current (µA) and charge (µC per phase) as a function of the number of sites stimulated in parallel for both 160 and 395 µm diameter electrodes. A 2 (electrode size: 160 µm diameter, 395 µm diameter) x 7 (number of sites: 1, 2, 4, 6, 8, 10 and 12 sites; Note data from parallel stimulation of 3 sites unavailable for 395 µm diameter) univariate ANOVA was performed to assess the interaction between electrode size and number of sites stimulated in parallel within a row. A significant main effect of number of sites was found [$F(6,114) = 8.59$, $p < 0.001$, $\eta^2 = 0.3$]. For both electrode sizes, thresholds from parallel stimulation of 12 sites (full rows; 160 µm, 39 rows in 7 eyes, 0.44±0.02 µC; 395 µm, 7 rows in 7 eyes, 0.31±0.04 µC) were higher than those from parallel stimulation of 6 sites (half-rows; 160 µm, 24 half-rows in 6 eyes, 0.24±0.02 µC; 395 µm, 8 half-rows in 7 eyes, 0.2±0.04 µC) which in turn were higher than those from stimulation of single sites (160 µm, 1 site in 1 eye, 0.06 µC; 395 µm, 14 sites in 7 eyes, 0.14±0.02 µC). Thresholds were not found to be dependent on electrode size and the interaction between electrode size and number of sites was not significant ($p > 0.05$). When converted to charge density values, the 395 µm diameter electrode sites required much lower charge densities to reach threshold compared to the 160 µm diameter electrode sites ($p < 0.001$).

Effect of Pulse Width:

Figure 7 depicts the changes observed in threshold current (figure 7A-C, data fitted with 2 parameter hyperbolic decay function) and threshold charge (figure 7D-F, data fitted with linear regression), with increasing pulse widths (composite strength-duration curves) for 160 µm and 395 µm diameter electrode sites. We were not able to determine rheobase currents and chronaxies, owing to limited pulse width data and a maximum employed pulse width of 500 µs.

However, we observed that threshold current for rows, half-rows and single sites reduced with increasing pulse widths as expected (figure 7A-C). When converted to charge per phase, thresholds tended to increase linearly with increasing pulse widths for the range of pulse widths used in this study. This effect was mostly exhibited by sites with 395 µm diameter (open circles; figure 7D, 395 µm diameter rows, $r^2 = 0.74$, Slope = 0.39; figure 7E, 395 µm diameter half-rows, $r^2 = 0.76$, Slope = 0.23; figure 7F, 395 µm diameter single sites, $r^2 = 0.88$, Slope = 0.25). Electrode sites with 160 µm diameters (filled circles) did not exhibit much change in charge thresholds with increasing pulse widths (figure 7D, 160 µm diameter rows, $r^2 = 0.02$, Slope = 0.04; figure 7E, 160 µm diameter half-rows, $r^2 = 0.09$, Slope = 0.08).

Amplitude and Latency Gradients

In order to compare the changes in response amplitudes with increasing stimulus levels across all animals (slopes of the input-output functions or gain), we calculated the dB change in amplitude per dB increase in current (µA) for electrical stimulation, and the dB change in amplitude per dB increase in flash brightness (cd/m^2) for visual stimulation. For visual stimulation, amplitude gradients ranged between 0.11-0.4 (0.2±0.04). For electrical stimulation, mean amplitude gradients for stimulation of rows were 1.24±0.26 and 0.7±0.18 for 160 µm and 395 µm diameter sites respectively, and for stimulation of half-rows were 1.33±0.14 and 0.84±0.14 for 160 µm and 395 µm diameter sites respectively. A 2 (electrode size: 160 µm diameter, 395 µm diameter) x 2 (number of sites: rows, half-rows) univariate ANOVA revealed that amplitude gradients did not significantly depend on electrode size, the number of sites stimulated in parallel or the interaction between the two factors ($p > 0.05$).

Latency gradients were calculated as change in ms per dB increase in stimulus intensity (cd/m^2 or µA). Latencies of the evoked responses decreased with increased flash brightness (0.53±0.14 ms per dB). However, with electrical stimulation, the latency gradients were smaller. For stimulation of sites with 160 µm diameter, the mean latency gradient was 0.24±0.15 ms decrease per dB

increase in current while for sites with 395 μm diameter, latencies slightly increased with increasing current (0.1±0.03 ms increase per dB). Similar to amplitude gradients, latency gradients were not dependent on electrode size or the number of sites within a row stimulated in parallel (2 X 2 ANOVA; $p > 0.05$).

Comparisons between Multiunit Activity and Evoked Responses

Although the majority of the electrophysiological data analysed in this study were cortical evoked potentials, in one animal we also recorded multiunit activity in response to both visual and electrical stimulation. Figure 8 shows a representative multiunit response from a single trial of a visual flash stimulus and a single trial of electrical stimulation of a full row of electrode sites. Unlike evoked responses, with multiunit activity we were able to clearly discern two spike responses separated in time (early and late responses), seen with both visual and electrical stimulation. The latency of the early response matched those of the evoked responses when compared at the same stimulus intensities, while latency of the late response was approximately 80 ms and 50 ms from visual and electrical stimulation respectively. Further, threshold of the multiunit activity (data not shown) was comparable to the thresholds of the evoked responses seen in this study.

Discussion:

The aim of the present study was to evaluate the effectiveness of varying a range of stimulus parameters and electrode geometry for electrical stimulation of the retina using suprachoroidal electrodes. We assessed the effect of: site of return electrode placement; electrode size; number of sites stimulated in parallel within a row; and pulse width on thresholds of evoked responses from the primary visual cortex. We also characterized the changes in electrode impedance in response to implantation. Our results provide valuable insights into the design parameters for retinal stimulation using suprachoroidal electrodes.

Electrode Impedance

Our results show that electrode impedances recorded *in vivo* were several times larger than those recorded *in vitro.* These data indicate that *in vivo* impedances were dominated by the choroidal tissue overlaying the electrodes or blood clots as a result of some insertion trauma, as opposed to the changes occurring on the electrode-tissue interface. A similar effect has been reported for an epiretinal array, where impedances recorded on the inner surface of the retina in porcine cadaver eyes were much higher than those recorded in the vitreous humour (Shah *et al* 2007). We also found that *in vivo* impedances were stable or progressively increased as a function of time. It should be noted that similar instabilities in impedances during the first few weeks after epiretinal implantations are not uncommon (de Balthasar *et al* 2008) and are also seen with cochlear implants (Shepherd *et al* 1990, Xu *et al* 1997). It is unclear at this stage as to how long-term mechanical stability of the electrode array within the suprachoroidal surgical pocket will affect impedances and cortical response thresholds. Given that the array is sandwiched between two tissue layers (sclera and choroid) we postulate that long-term stability may not be a major issue. We are currently conducting a chronic study to determine the long-term stability of the suprachoroidal array. In contrast, epiretinal arrays have been found to drift back into the vitreous humour over time, resulting in the reduction of electrode impedances and increases in perceptual

thresholds (de Balthasar *et al* 2008). The progressive increase in impedance over the duration of the experiments seen in our study may reflect settling of the arrays on the choroid or biological and electrochemical changes at the electrode-tissue interface. This study does not address the long term changes that commonly occur at the electrode-tissue interface with chronic implantation and electrical stimulation such as formation of fibrous tissue layers and gliosis (Duan *et al* 2004, Grill and Mortimer 1994). As expected, the impedances of larger diameter electrode sites were lower than those of small diameter sites also consistent with previously reported results for epiretinal implantations in humans (de Balthasar *et al* 2008).

Cortical Evoked Responses

Evoked responses in the primary visual cortex to both visual and electrical stimulation were similar in shape with the exception of longer latencies with visual stimulation compared to electrical stimulation. Electrically evoked latencies in this study (7.7±0.3 ms) were comparable to the latencies reported previously for epiretinal stimulation in cats (10-20 ms for early component, Eckhorn *et al* 2006; approximately 10 ms, Elfar *et al* 2009), suprachoroidal stimulation in cats and rabbits using similar arrays (9±1 ms, Sakaguchi *et al* 2004; 10.5±0.6 ms, Wong *et al* 2009; 16±2 ms, Nakauchi *et al* 2005), and extraocular stimulation in cats (approximately 8 ms, Chowdhury *et al* 2005). Moreover, the latency of the early multiunit response in this study matched well to the latencies of the evoked responses and confirmed that the recorded evoked responses were as a result of activation of the visual cortex. In our study, the mean latencies of the electrically evoked responses were more than 12-20 ms shorter than the visually evoked responses, strongly suggesting that suprachoroidal stimulation can directly activate cells within the middle and inner retina bypassing the photoreceptors, although it is still unknown as to which population of cells are primarily activated by electrical stimulation. It is interesting to note that all the evoked responses obtained in our study only consisted of a single positive peak. Other studies using suprachoroidal, extraocular or epiretinal stimulation in cats (Elfar *et al* 2009, Chowdhury *et*

al 2005, Wong *et al* 2009), as well as the multiunit activity obtained in our study (figure 7), have shown the presence of two positive-going cortical responses (an early and late component). It is posited that the early component arises from direct activation of retinal ganglion cells while the late component is attributed to indirect activation of bipolar cells and/or photoreceptors (Elfar *et al* 2009). Furthermore, the presence of the various peaks in the evoked responses as well as their polarities have been shown to be dependent on the placement and/or depth of the recording electrode on the visual cortex (Elfar *et al* 2009, Wong *et al* 2009). The absence of a second peak in our study is likely due to the different techniques used for recordings amongst the studies. The most obvious difference was that we recorded the evoked responses using a macroelectrode placed on the duramater above the surface of the visual cortex as opposed to multichannel recording grids or penetrating electrodes as used in other studies. It remains unknown as to how these early and late components relate to prosthetic vision perception as retinitis pigmentosa patients who form one of the main target groups for retinal prostheses can have a significant percentage of cells within the inner retinal layers and associated ganglion circuitry still present (Santos *et al* 1997, Humayun *et al* 1999b).

The thresholds of the evoked responses in our study from monopolar stimulation of single 395 µm diameter sites using 500 µs pulse widths (141±16 nC) were higher than those reported previously for hexagonal return suprachoroidal stimulation in cats (76±9 nC, Wong *et al* 2008, 2009, 400 µs cathodic-first biphasic pulses). The thresholds reported in the present study are likely to be overestimated due to the coarse step size of the current increments we used for the input-output functions (i.e. our lowest measurable threshold was either 100 or 200 µA). Additionally, the differences in signal-to-noise ratio as a result of the number of averages performed (25 in our study, 300 in the study by Wong *et al*) could be expected to result in the higher thresholds seen in our study. Furthermore, the thresholds found in our study were also higher than those reported previously with monopolar stimulation in rabbits (28±5 nC, Nakauchi *et al* 2005, monopolar stimulation with 500 µs anodic monophasic pulses; 33±16 nC, Sakaguchi

et al 2004, monopolar stimulation with 500 µs cathodic-first biphasic pulses). These differences likely relate to differences in recording techniques, species, and/or the design and positioning of the stimulating electrode array. For example, we used a platinum macroelectrode for recordings on the surface of the visual cortex as opposed to other studies that either used screws (Sakaguchi *et al* 2004, Nakauchi *et al* 2005) or multichannel electrode grids (Wong *et al* 2008, 2009). Nevertheless, the charge thresholds in our study from stimulation of both large and small diameter single electrode sites were lower than those found to damage the rabbit retina with suprachoroidal stimulation using 500µs pulses (approximately 300-500 nC; Nakauchi *et al* 2007). In addition, charge densities required to reach threshold in this study were lower than the set maximum non-gassing limit of 300 µC/cm^2 per phase, also deemed to be safe for stimulation of platinum electrodes (Brummer and Turner 1977). Thresholds from parallel stimulation of some combinations of multiple sites within a row involved higher charge per phase however, in these cases the charge would spread over multiple electrodes resulting in lower charge per electrode and even lower charge densities compared to stimulation of single sites.

Current thresholds were found to decrease while charge thresholds were found to linearly increase with increasing pulse widths, consistent to what has been previously reported for suprachoroidal (Wong *et al* 2009) and epiretinal (Shyu *et al* 2006) stimulation. Shorter pulses would enable fast sequential stimulation of sites (40-50 Hz) on a reasonably large footprint electrode array to avoid flicker and enable quicker delivery of charge to reduce power requirements. On the other hand, wider pulses would require less current to activate the retina and therefore require significantly lower voltages, particularly for stimulation of larger electrode sites at the expense of slightly higher charge per phase. Cortical thresholds were not dependent on the site of placement of the return electrode for monopolar stimulation. A similar effect of return placement on cortical thresholds has been found with epiretinal stimulation in rabbits (Shah *et al* 2006). The vitreous return, in theory, should direct most of the current flow through the retina and into the vitreous humour (trans-retinal stimulation) and therefore should be more efficacious, compared to a

suprachoroidally placed return. On the other hand, the suprachoroidal placement of the return involves a simpler and safer implantation site, suggesting the possibility of choosing a suprachoroidal return electrode over the vitreous return for the final implant design. However, it will be important to systematically assess the effect of return placement on localisation of retinal activation by acquiring multiunit activity from several recording sites in the visual cortex in response to retinal stimulation. These studies will help determine the most suitable return placement for the final implant design.

Cortical thresholds were not dependent on the electrode sizes (tested separately for rows, half-rows and single sites) tested in this study, consistent with what has been reported in patients with long-term epiretinal implantations of electrode arrays that had 260 μm and 520 μm diameter sites (de Balthasar *et al* 2008). Further, our data indicated that both the amplitude and latency gradients of the evoked responses as a function of current were not dependent on electrode size. Since amplitude growth functions could be an indication of the change in perceptual brightness associated with changes in stimulus current, it will be important to investigate if electrode size will affect overall perceived brightness. Smaller electrodes did not provide any benefit in terms of thresholds while often failing to evoke neural activity within electrochemically safe limits. This finding, together with the advantage of larger sites having lower impedances and lower charge densities, suggest that the use of relatively wide pulse widths and larger electrodes are the ideal combination for minimizing voltage requirements for a suprachoroidal stimulator. Ultimately, larger electrodes may limit the resolution and acuity achieved with the implant resulting in a compromised balance between stimulator compliance voltage, low power requirements and highest resolution achievable with suprachoroidal prostheses. This will only be resolved via psychophysical experiments in blind patients implanted with suprachoroidal electrode arrays.

Our results showed that threshold charge for sites stimulated in parallel within a row were higher than those for single electrode sites (approximately 2-6 fold increase from single sites to rows). However the increase in thresholds as a function of the number of sites stimulated in parallel was

less than expected from summing thresholds from sequentially stimulating sites within a row (assumed as approximately 12 times threshold of single site). Particularly for larger electrodes, thresholds did not increase to a large extent when stimulating rows compared to single sites. Further, the amplitude and latency growth functions did not depend on the number of sites stimulated in parallel within a row. Together these data are compatible with convergence within the visual system for the perception of edges (Marr and Hildreth 1980). In addition, since the impedance of a single site would be much higher than that of multiple parallel sites, higher voltages would be required to inject the same amount of charge when stimulating one site compared to when stimulating multiple parallel sites. As a result, the technique of stimulating multiple sites in parallel would also result in a marked reduction in voltage compliance limits required by a suprachoroidal retinal stimulator.

Psychophysical studies in humans fitted with epiretinal implants with 16-site electrode arrays (Caspi *et al* 2009, Humayun *et al* 1999a) have shown that fast sequential stimulation and simultaneous stimulation of a row or column of electrode sites can elicit the percept of a continuous flicker-free horizontal or vertical line rather then a series of pixels. In addition, Rizzo *et al* (2003) using multiple current sources were able to simultaneously stimulate groups of electrode sites in human patients which were perceived as distinct patterns. The "pattern-like" stimulation could be easily implemented by stimulating multiple sites in parallel using only one current source (Elfar *et al* 2009; present study). It is important to note that in the case of cochlear implants, adverse effects of channel interaction between simultaneously stimulated electrode sites using multiple current sources can arise from the summation of their electric fields (Bierer and Middlebrooks 2004). Current pulses are therefore typically delivered in a sequential manner whereby stimulation is delivered to a single electrode at a time (Wilson *et al* 1991, Black *et al* 1981, Townshend and White 1987). It remains to be seen whether sequential stimulation strategies can be adopted for retinal prostheses or the technique of simultaneous parallel

stimulation employed in this study proves to be more beneficial along with reduced voltage requirements.

In conclusion, our results demonstrate that retinal stimulation via the suprachoroidal approach is capable of evoking activity in the visual cortex using stimuli operating within the known safety limits for electrical stimulation of neural tissue with platinum electrodes. The results suggest that for monopolar stimulation the combination of large diameter electrodes, wide pulse widths and parallel stimulation of aligned sites will markedly reduce voltage requirements for a suprachoroidal stimulator.

Acknowledgements:

The authors wish to thank Mark McCombe for assistance with surgeries, David Ng for designing the flexible electrode arrays, Tom Landry and David Perry for assistance with data collection, and Meera Ulaganathan, Rebecca Argent and Rodney Millard for technical assistance. This work was performed at the Bionic Ear Institute at St. Vincent's hospital, and the Department of Otolaryngology, University of Melbourne at the Royal Victorian Eye and Ear Hospital. Funding was provided by the Ian Potter Foundation and John T Reid Charitable Trusts. The Bionic Ear Institute acknowledges the support it receives from the Victorian Government through its Operational Infrastructure Support Program.

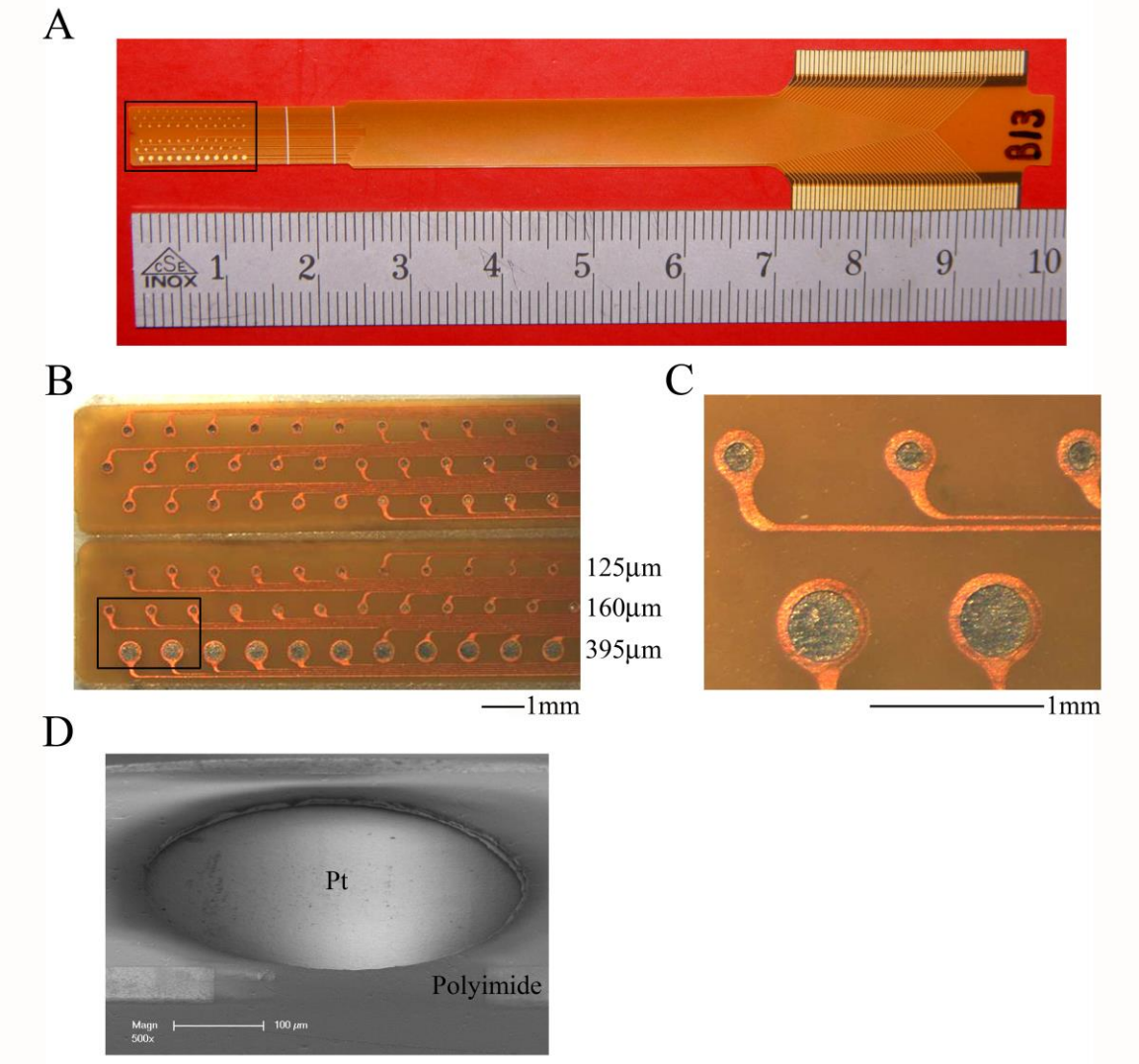

Figure 1. Suprachoroidal Flexible Electrode Array. (A) Polyimide based suprachoroidal flexible electrode array with 72 gold plated electrode sites. Highlighted region in (A) is shown in (B). Sites were arranged in a 6 row x 12 electrode site configuration and electroplated with platinum. Each row had electrode sites of different diameters (Row 4 – 125 µm diameter; Rows 1:3, Row 5 – 160 µm diameter; Row 6 – 395 µm diameter). Highlighted region in (B) is shown in (C). (D) Scanning electron micrograph showing the platinum (Pt) plated electrode surface and the Polyimide substrate.

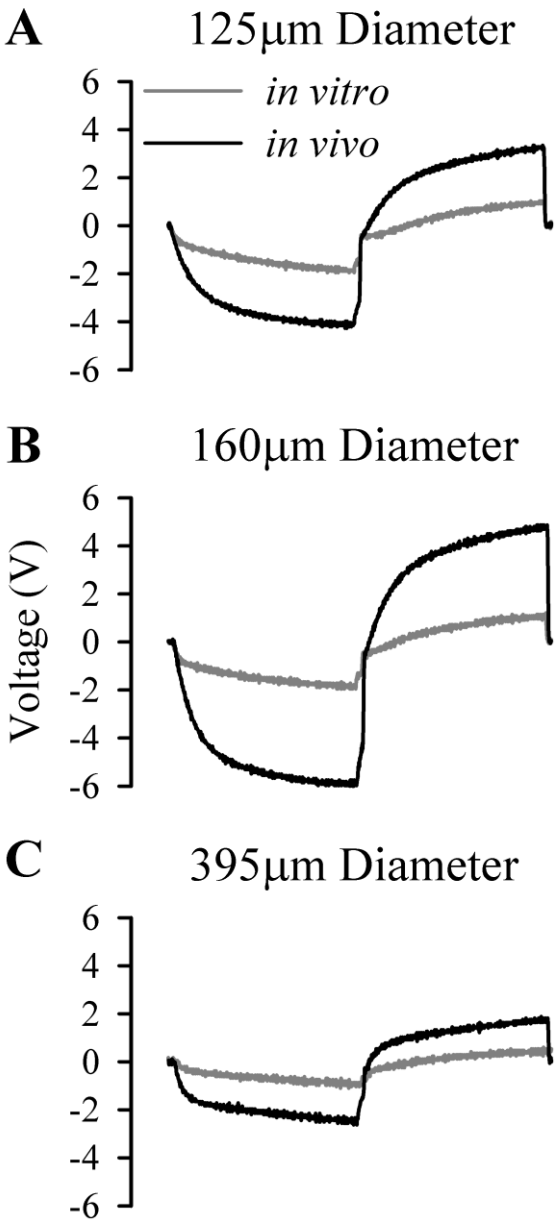

Figure 2. Voltage waveforms for impedance calculations. (A) Voltage waveforms recorded in vitro (gray) and 40 hours post-op in vivo (black) by stimulating a single 125 µm diameter electrode site with a charge-balanced biphasic pulse (100 µA, 250 µs per phase). Impedance was calculated by dividing the magnitude of the peak voltage recorded in the leading cathodic phase of the pulse by the injected current. Similar data for a 160 µm diameter and a 395 µm diameter electrode site using a 200 µA (250 µs per phase) current pulse shown in (B) and (C) respectively.

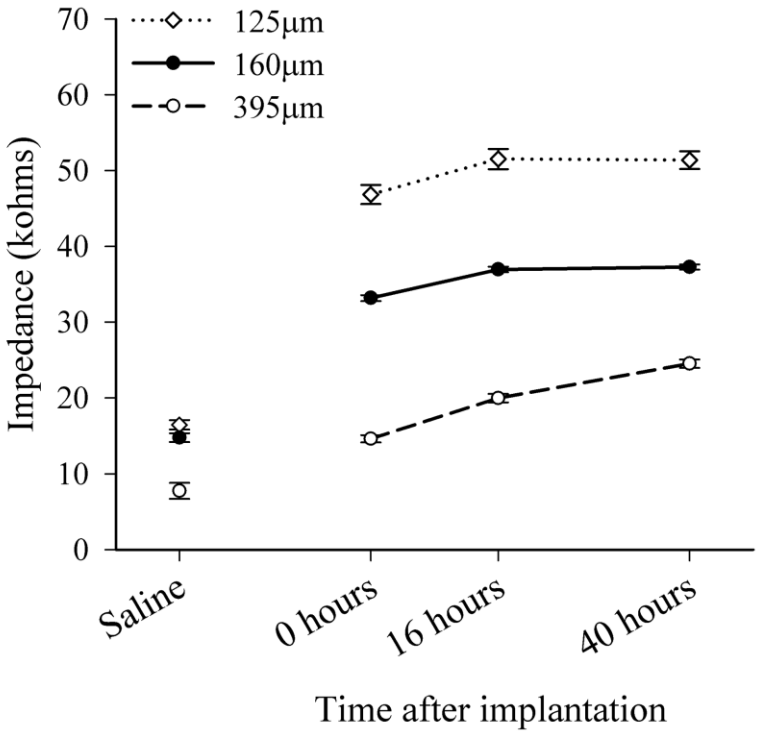

Figure 3. Electrode Impedances. Electrode impedances recorded in vitro (saline) and in vivo as a function of time post-op for the 125 µm, 160 µm and the 395 µm diameter electrode sites (suprachoroidal and vitreous return data combined).

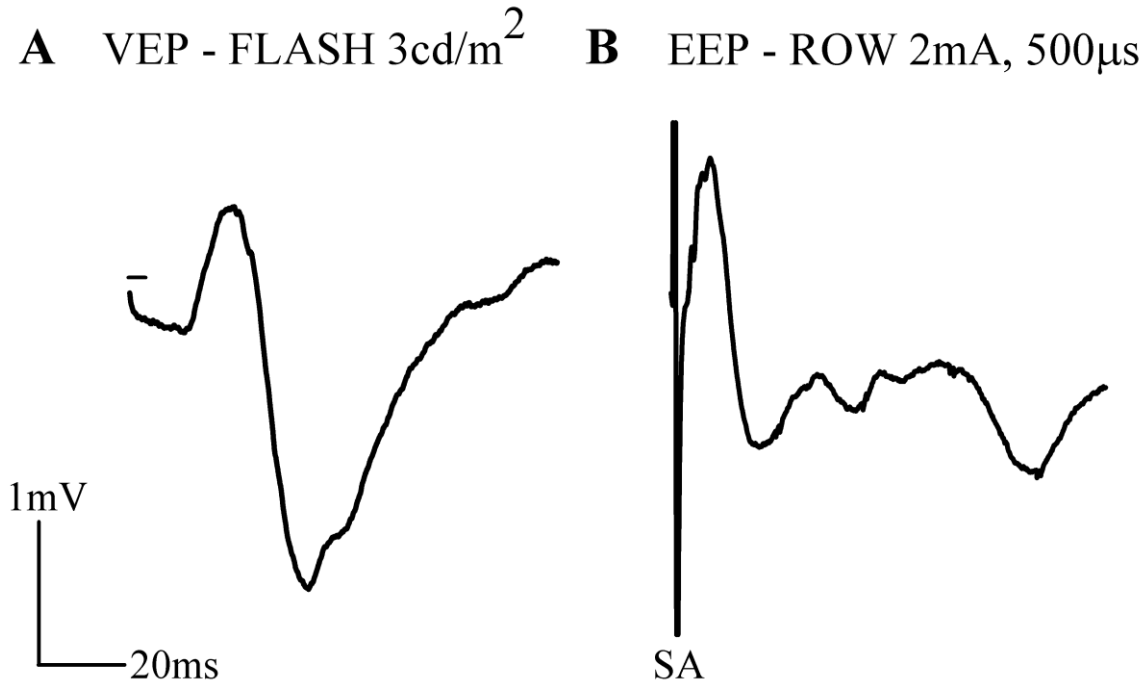

Figure 4. Example of Visual- (VEP) and Electrically-Evoked Cortical Potential (EEP). (A) Primary visual cortex average evoked response to a 3 cd/m^2 bright flash (25 trials). Solid flat line indicates duration of the flash stimulus (B) Average evoked response to electrical stimulation of a row of 395 µm diameter electrode sites at 2 mA using a 500 µs pulse width (25 trials). Note stimulus artefact (SA) at 0 ms with electrical stimulation.

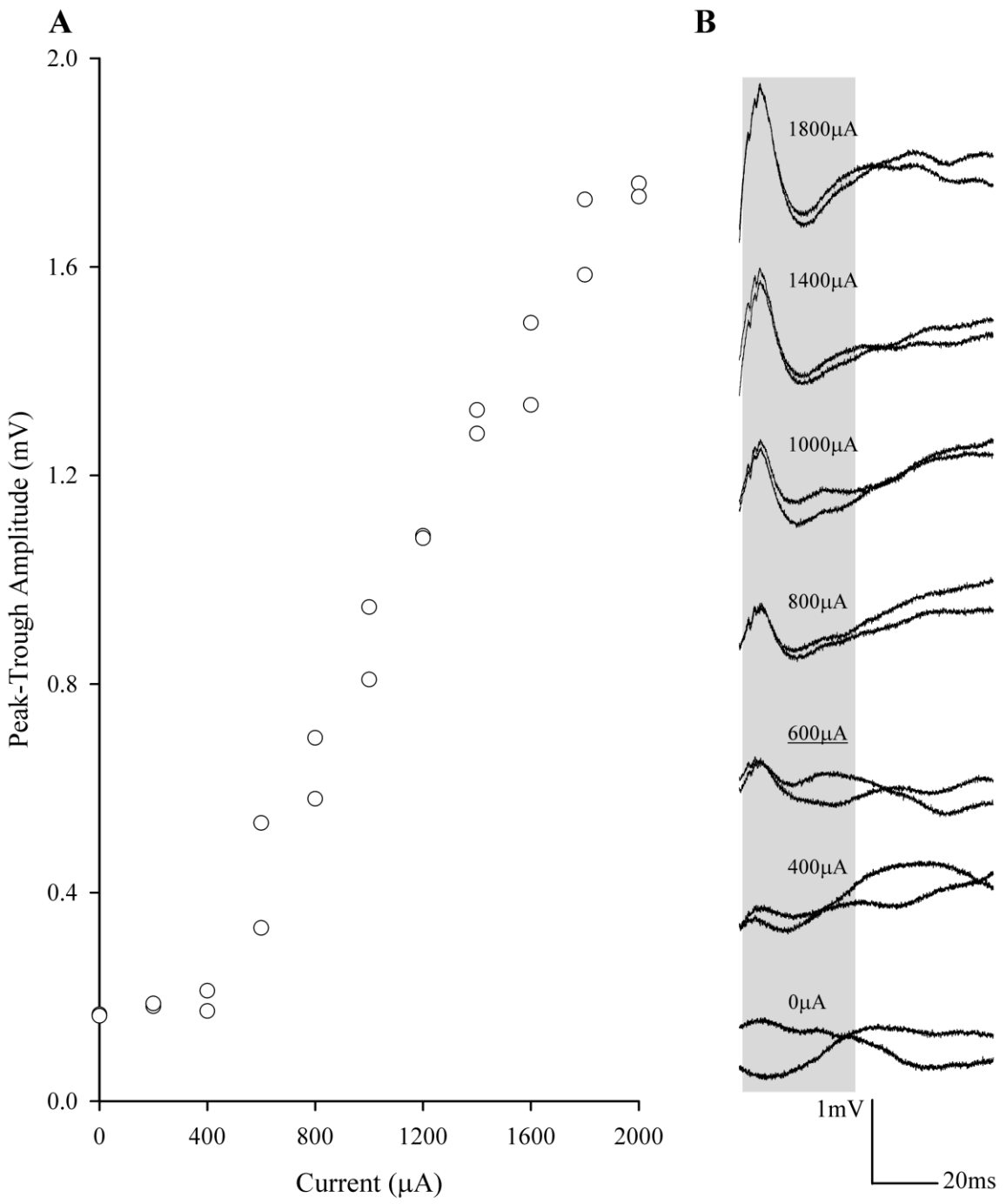

Figure 5. Amplitude Gradient. (A) Peak-Trough amplitude of the average evoked response to charge-balanced electrical stimulation of a row of 395 µm diameter electrode sites as a function of stimulus current. Data were collected using 500 µs per phase pulses and the vitreous return for stimulation. (B) Average evoked responses whose amplitudes are shown in (A) at various stimulus currents for two repeats of the stimulus input-output function. Stimulus artefacts have been

removed for display purposes. Shaded region denotes time window for measuring peak-trough amplitudes (2-30 ms from stimulus onset). Threshold determined as 600 μA (300 nC per phase).

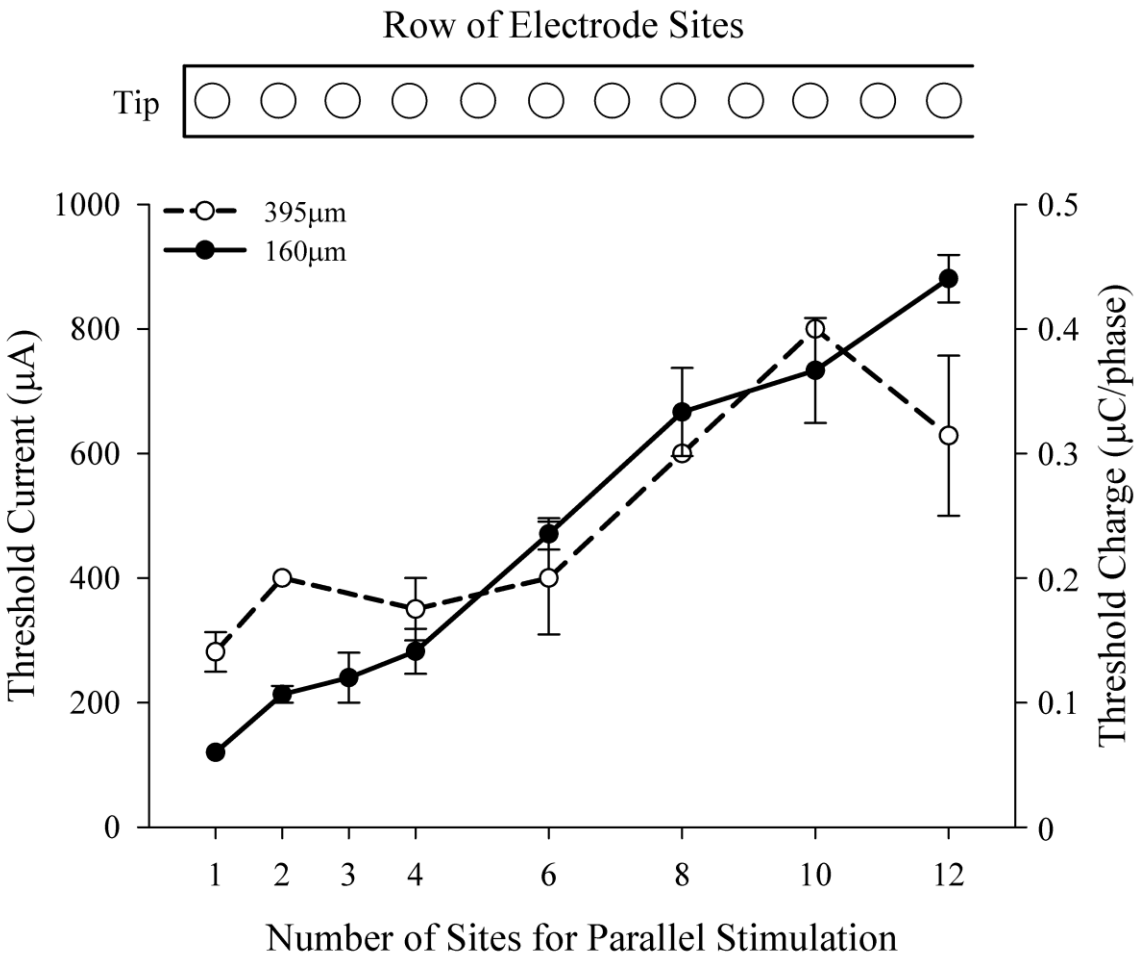

Figure 6. Thresholds and Number of Sites. Mean current and total charge per phase thresholds as a function of the number of sites stimulated in parallel within a row for the 160 µm diameter sites using a 500 µs pulse width (solid line, filled circles; data using vitreous and suprachoroidal return combined). Similar data is presented for the 395 µm diameter sites (dashed line, open circles). Schematic of a row of 12 electrode sites from tip shown as a reference for parallel stimulation.

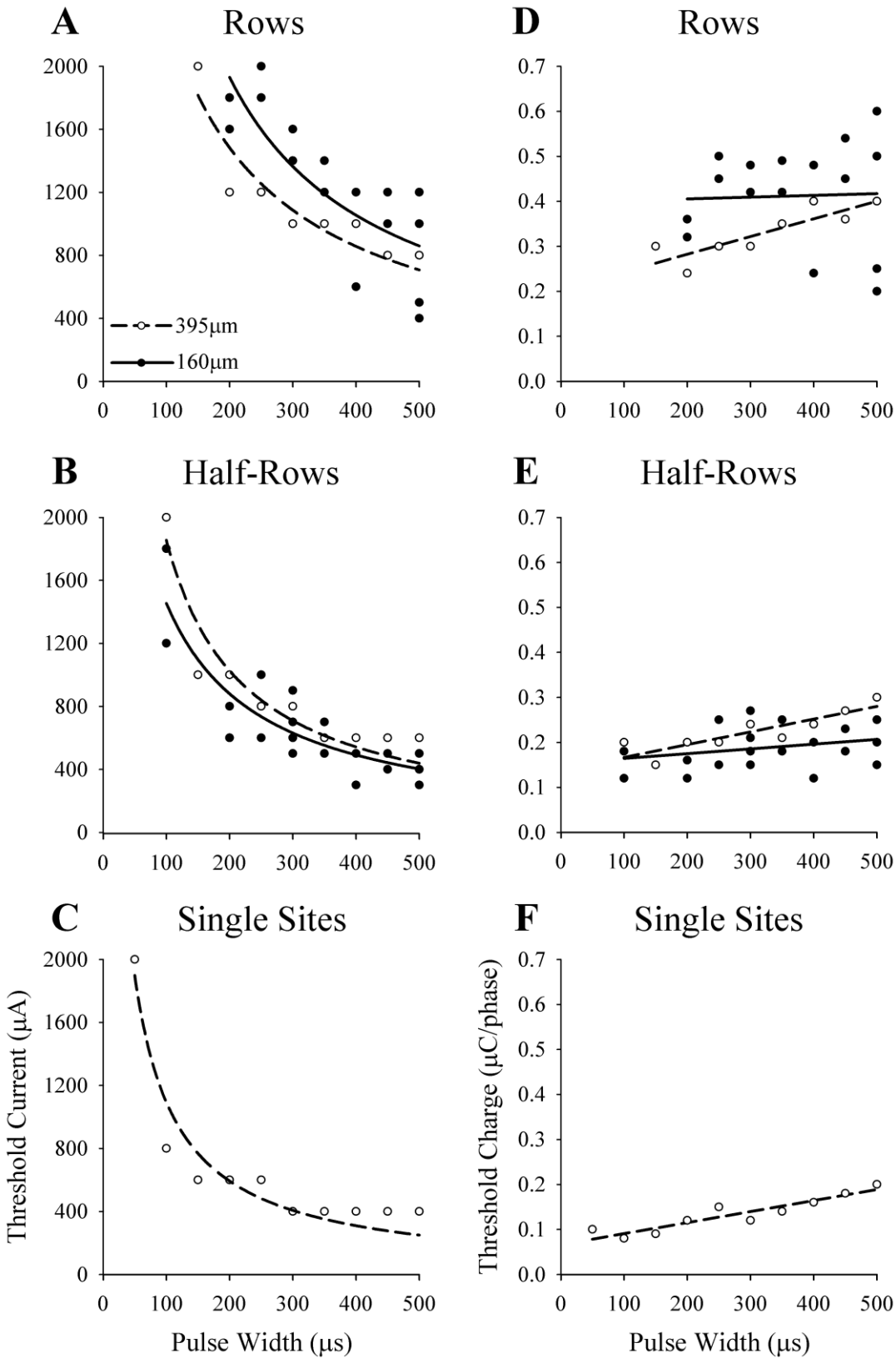
A
Rows
D
Rows
B
Half-Rows
E
Half-Rows
C
Single Sites
F
Single Sites
395µm
160µm
Threshold Current (µA)
Threshold Charge (µC/phase)
Pulse Width (µs)
Pulse Width (µs)

*Figure 7. Thresholds and Pulse Width. (A) Composite strength-duration curves for electrical stimulation of rows of electrode sites using pulse widths from 100-500 µs per phase. Data points have been fitted using a 2 parameter hyperbolic decay function [y = (a*b)/(b+x)] where a and b are constants. Similar data as (A) for examples of half-rows (B) and a single electrode site (C). Corresponding threshold charge per phase as a function of pulse width is shown in (D-F). Data points have been fitted using linear regression. Filled circles (solid lines for regression) and open circles (dashed lines for regression) show data from 160 µm and 395 µm diameter sites respectively.*

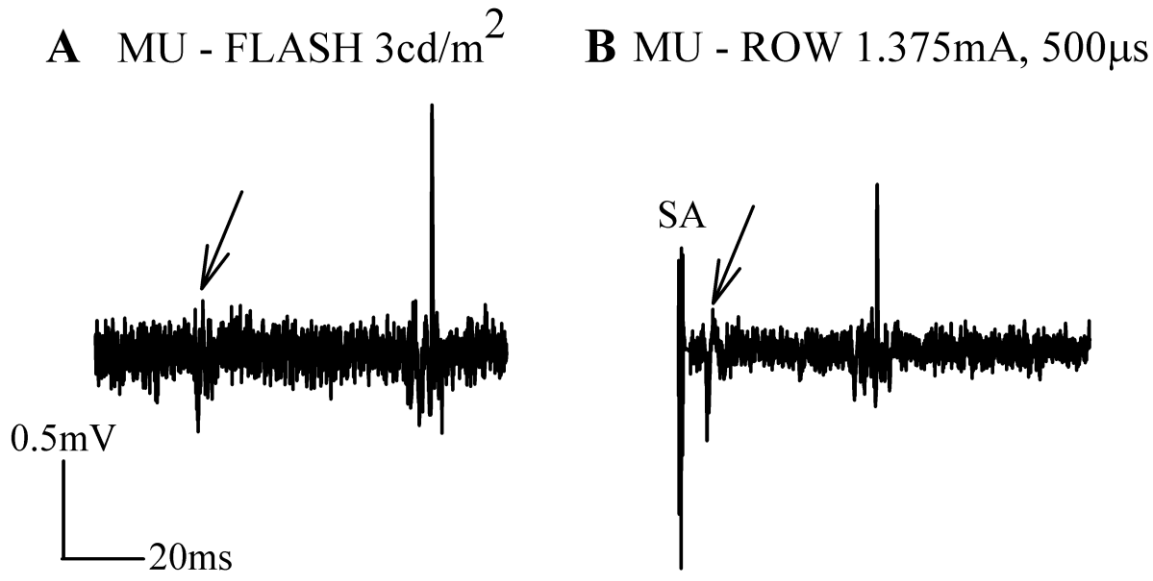

Figure 8. Multiunit Example. (A) Example of multiunit (MU) activity recorded from the primary visual cortex in response to a single full-field flash (3 cd/m^2 brightness). (B) Same multiunit responding to a single trial of electrical stimulation of a half-row of 160 µm diameter electrode sites (1.375 mA, 500 µs per phase). Note presence of both early (arrows) and late components of multiunit activity with visual and electrical stimulation. The latency of the cortical evoked potentials presented in this study matched the early multiunit component. Stimulus artefact (SA) from electrical stimulation present at 0 ms.

References:

Allen, P. J., McCombe, M. F., Luu, C. D., Villalobos, J., Shivdasani, M. N., Fallon, J. B., Lovell, N. H., Suaning, G. J., Williams, C. E. and Guymer, R. H. (2009) In *Retina Congress*New York.

Bierer, J. A. and Middlebrooks, J. C. (2004) *J Assoc Res Otolaryngol,* **5,** 32-48.

Black, R. C., Clark, G. M. and Patrick, J. F. (1981) *IEEE Trans Biomed Eng,* **28,** 721-5.

Brown, J. S., Flitcroft, D. I., Ying, G. S., Francis, E. L., Schmid, G. F., Quinn, G. E. and Stone, R. A. (2009) *Invest Ophthalmol Vis Sci,* **50,** 5-12.

Brummer, S. B. and Turner, M. J. (1977) *IEEE Trans Biomed Eng,* **24,** 59-63.

Caspi, A., Dorn, J. D., McClure, K. H., Humayun, M. S., Greenberg, R. J. and McMahon, M. J. (2009) *Arch Ophthalmol,* **127,** 398-401.

Chow, A. Y., Pardue, M. T., Chow, V. Y., Peyman, G. A., Liang, C., Perlman, J. I. and Peachey, N. S. (2001) *IEEE Trans Neural Syst Rehabil Eng,* **9,** 86-95.

Chowdhury, V., Morley, J. W. and Coroneo, M. T. (2005) *J Clin Neurosci,* **12,** 574-9.

de Balthasar, C., Patel, S., Roy, A., Freda, R., Greenwald, S., Horsager, A., Mahadevappa, M., Yanai, D., McMahon, M. J., Humayun, M. S., Greenberg, R. J., Weiland, J. D. and Fine, I. (2008) *Invest Ophthalmol Vis Sci,* **49,** 2303-14.

Drasdo, N. and Fowler, C. W. (1974) *Br J Ophthalmol,* **58,** 709-14.

Duan, Y. Y., Clark, G. M. and Cowan, R. S. (2004) *Biomaterials,* **25,** 3813-28.

Eckhorn, R., Wilms, M., Schanze, T., Eger, M., Hesse, L., Eysel, U. T., Kisvarday, Z. F., Zrenner, E., Gekeler, F., Schwahn, H., Shinoda, K., Sachs, H. and Walter, P. (2006) *Vision Res,* **46,** 2675-90.

Elfar, S. D., Cottaris, N. P., Iezzi, R. and Abrams, G. W. (2009) *J Neurosci Methods,* **180,** 195-207.

Fallon, J. B., Irvine, D. R. and Shepherd, R. K. (2009) *J Comp Neurol,* **512,** 101-14.

Fujikado, T., Morimoto, T., Kanda, H., Kusaka, S., Nakauchi, K., Ozawa, M., Matsushita, K., Sakaguchi, H., Ikuno, Y., Kamei, M. and Tano, Y. (2007) *Graefes Arch Clin Exp Ophthalmol,* **245,** 1411-9.

Grill, W. M. and Mortimer, J. T. (1994) *Ann Biomed Eng,* **22,** 23-33.

Hubel, D. H. and Wiesel, T. N. (1959) *J Physiol,* **148,** 574-91.

Humayun, M. S., de Juan, E., Jr., Weiland, J. D., Dagnelie, G., Katona, S., Greenberg, R. and Suzuki, S. (1999a) *Vision Res,* **39,** 2569-76.

Humayun, M. S., Prince, M., de Juan, E., Jr., Barron, Y., Moskowitz, M., Klock, I. B. and Milam, A. H. (1999b) *Invest Ophthalmol Vis Sci,* **40,** 143-8.

Kanda, H., Morimoto, T., Fujikado, T., Tano, Y., Fukuda, Y. and Sawai, H. (2004) *Invest Ophthalmol Vis Sci,* **45,** 560-6.

Leuenberger, J., Millard, R. E. and Williams, C. E. (2008) In *Medical Bionics - a new paradigm for human health*Lorne, Victoria, Australia.

Majji, A. B., Humayun, M. S., Weiland, J. D., Suzuki, S., D'Anna, S. A. and de Juan, E., Jr. (1999) *Invest Ophthalmol Vis Sci,* **40,** 2073-81.

Marr, D. and Hildreth, E. (1980) *Proc R Soc Lond B Biol Sci,* **207,** 187-217.

Nakauchi, K., Fujikado, T., Kanda, H., Kusaka, S., Ozawa, M., Sakaguchi, H., Ikuno, Y., Kamei, M. and Tano, Y. (2007) *J Neural Eng,* **4,** S50-7.

Nakauchi, K., Fujikado, T., Kanda, H., Morimoto, T., Choi, J. S., Ikuno, Y., Sakaguchi, H., Kamei, M., Ohji, M., Yagi, T., Nishimura, S., Sawai, H., Fukuda, Y. and Tano, Y. (2005) *Graefes Arch Clin Exp Ophthalmol,* **243,** 169-74.

Rizzo, J. F., 3rd, Wyatt, J., Loewenstein, J., Kelly, S. and Shire, D. (2003) *Invest Ophthalmol Vis Sci,* **44,** 5362-9.

Sakaguchi, H., Fujikado, T., Fang, X., Kanda, H., Osanai, M., Nakauchi, K., Ikuno, Y., Kamei, M., Yagi, T., Nishimura, S., Ohji, M. and Tano, Y. (2004) *Jpn J Ophthalmol,* **48,** 256-61.

Santos, A., Humayun, M. S., de Juan, E., Jr., Greenburg, R. J., Marsh, M. J., Klock, I. B. and Milam, A. H. (1997) *Arch Ophthalmol*, **115,** 511-5.

Shah, H. A., Montezuma, S. R. and Rizzo, J. F., 3rd (2006) *Exp Eye Res*, **83,** 247-54.

Shah, S., Hines, A., Zhou, D., Greenberg, R. J., Humayun, M. S. and Weiland, J. D. (2007) *J Neural Eng*, **4,** S24-9.

Shepherd, R. K., Franz, B. K. H. and Clark, G. M. (1990) In *Cochlear Prostheses*(Eds, Clark, G. M., Tong, Y. C. and Patrick, J. F.) Churchill-Livingstone, Edinburgh, pp. 69-98.

Shyu, J. S., Maia, M., Weiland, J. D., Ohearn, T., Chen, S. J., Margalit, E., Suzuki, S. and Humayun, M. S. (2006) *IEEE Trans Neural Syst Rehabil Eng*, **14,** 290-8.

Townshend, B. and White, R. L. (1987) *IEEE Trans Biomed Eng*, **34,** 891-7.

Tusa, R. J., Palmer, L. A. and Rosenquist, A. C. (1978) *J Comp Neurol*, **177,** 213-35.

Wilson, B. S., Finley, C. C., Lawson, D. T., Wolford, R. D., Eddington, D. K. and Rabinowitz, W. M. (1991) *Nature*, **352,** 236-8.

Wong, Y. T., Chen, S. C., Kerdraon, Y. A., Allen, P. J., McCombe, M. F., Morley, J. W., Lovell, N. H. and Suaning, G. J. (2008) *Conf Proc IEEE Eng Med Biol Soc*, **2008,** 1789-92.

Wong, Y. T., Chen, S. C., Seo, J. M., Morley, J. W., Lovell, N. H. and Suaning, G. J. (2009) *Vision Res.*

Xu, J., Shepherd, R. K., Millard, R. E. and Clark, G. M. (1997) *Hear Res*, **105,** 1-29.

Zhou, J. A., Woo, S. J., Park, S. I., Kim, E. T., Seo, J. M., Chung, H. and Kim, S. J. (2008) *J Biomed Biotechnol*, **2008,** 547428.